Design of A Wideband Miniature Dielectric-Filled Waveguide Antenna for Collision-Avoidance Radar

M. Hajian, D. P. Tran, and L. P. Ligthart

Institute Research Centre for Telecommunications–Transmission and Radar (IRCTR)
Delft University of Technology, Department of Electrical Engineering
Mekelweg 4, 2628 CD Delft, The Netherlands
Tel: +31 152781034; Fax: +31 152784046; E-mail: m.hajian@its.tudelft.nl

Abstract

This article presents a theoretical and experimental study of the design of a miniaturized wideband dielectric-filled waveguide (DFW) antenna. The operational frequency is X band, i.e., $9.0 \leq f \leq 10.5$ GHz. The desired bandwidth is 1.5 GHz. The antenna uses an air-gap matching network to reduce its high aperture reflection. In order to ease the integration with antenna circuits and to increase the bandwidth, two E-plane steps are used. The antenna is designed to have –3 dB beamwidths of 60° and 100° for the E- and H-plane patterns, respectively. An input reflection of less than –10 dB for the desired bandwidth is observed. The gain of the antenna is 7 dBi. A cross-polar level of less than –25 dB is achieved. This article discusses the mathematical model for input reflection, the design scenarios, and the experimental results.

Keywords: Dielectric antennas; waveguide antennas; road vehicle radar; wideband antennas; FM radar; CW radar

1. Introduction

The use of large wideband phased arrays, often consisting of thousands of elements, leads to the practical problems of cost, dimensions, bandwidth, and integration with antenna circuits. The trend toward development of antennas with conformal topology, that are lightweight, have superior performance, are low cost, and have easy maintenance plays an important role in antenna array design. In the past two decades, microstrip antennas [1-2] have been designed because of their advantages. However, they suffer from high cross polarization and narrow bandwidth. To overcome these disadvantages, the design criteria of microstrip antennas and waveguides have been combined, resulting in a dielectric-filled waveguide (DFW) antenna with low height. Such an antenna is called a microstrip-like antenna (MLA).

An MLA is a miniaturized DFW with dimensions smaller than half the free-space wavelength. Miniaturization is achieved by filling the waveguide with a dielectric material, and reducing its height. Reducing the height causes the antenna to exhibit high aperture reflections. In this case, analyzing the aperture admittance and reflection play crucial roles in designing an MLA [3]. An MLA is used for the IRCTR Collision Avoidance Radar.

The IRCTR Collision Avoidance Radar is designed for use on automatically guided vehicles. It is an FM-CW multi-static radar. This radar uses array antennas in a sparse form. Three antennas are used for transmission, and two are used for reception. Only one antenna transmits at a time. The prototype radar system is designed in the X band. The system will be up-converted to a frequency to the millimeter-wave band in the near future.

In the following sections, the specifications, the theoretical results for aperture reflection, the matching technique, the input reflection with two E-plane steps, and the measurement results are presented.

2. Specifications

Figure 1 shows the prototype IRCTR Collision Avoidance Radar system, and Table 1 gives the specifications of the MLA [4-5]. The arrows show the location of the antennas.

3. Aperture Dimensions

Figure 2 shows the geometry of the MLA aperture.

The total *half-power beamwidths* (HPBWs) in the principal E- and H-plane patterns are related to the aperture dimensions, a and b, according to [6]

 1045-9243/00/$10.00© 2000 IEEE

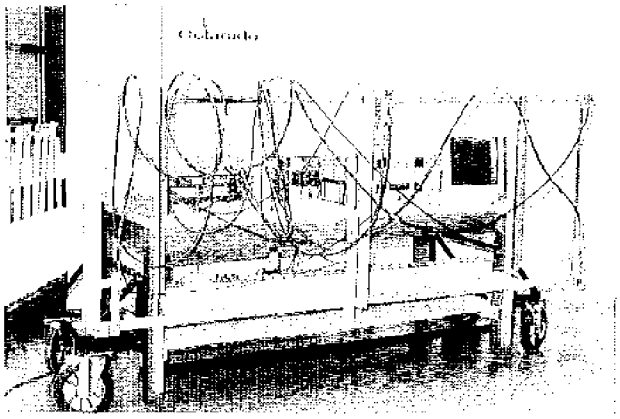

Figure 1. The IRCTR Collision Avoidance Radar System.

Table 1. The design parameters for the microwave-like antenna (MLA) at X band.

3 dB beamwidth	E plane: 60°; H plane: 100°
Center frequency	9.75 GHz
Bandwidth	1.5 GHz
Input reflection at the coax reference plane	$\Gamma_i \le -10$ dB for desired bandwidth
Maximum gain	≈ 7 dBi
Cross-polar level	< −25 dBi
Dielectric material	Rexolite: $\varepsilon_r = 2.53$
Sidelobe level	No sidelobe, $-90° \le \theta \le 90°$

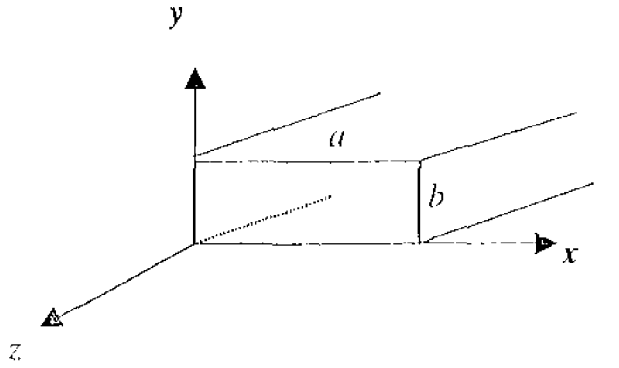

Figure 2. The MLA aperture in the (x, y, z) coordinate system.

$$\Theta_e = 2\theta_e = 114.6\sin^{-1}\left(\frac{0.443\lambda_0}{\sqrt{\varepsilon_r}\,b}\right)\text{degrees},$$
$$\Theta_h = 2\theta_h = 114.6\sin^{-1}\left(\frac{0.443\lambda_0}{\sqrt{\varepsilon_r}\,a}\right)\text{degrees}, \tag{1}$$

where a and b are the width and height of the aperture, λ_0 is the free-space wavelength, and ε_r is the dielectric constant of the material. The filling dielectric material is Rexolite. The dielectric constant is 2.53. Substituting the values of -3 dB beamwidth for the E- and H-plane patterns leads to $a \approx 17$ mm and $b \approx 11$ mm.

4. Aperture Reflection

It has been shown that when the height of an MLA is decreased, the aperture reflections will drastically increase. In the design process, the knowledge of the aperture admittance and its reflection are needed to design the antenna and its matching network. The MLA is excited by the symmetrical TE_{m0} modes. The problem is tackled using variational techniques, the boundary condition, energy conservation, and continuous tangential fields across the aperture. The element of the aperture admittance, Y_{ij}, is given by

$$Y_{ij} = Y_{ij} = \frac{2}{ab}\frac{1}{\omega\mu}\frac{1}{4\pi^2}\int_{-\infty}^{\infty}\int_{-\infty}^{\infty}\frac{\left(k^2 - k_x^2\right)}{k_z}c_0^2 c_i c_j\,dk_x dk_y,$$
$$c_0(k_y) = \frac{b\sin\left(k_y\frac{b}{2}\right)}{k_y\frac{b}{2}},$$
$$c_m(k_x) = \frac{2m\pi a j^{m+1}\cos\left(k_x\frac{a}{2}\right)}{(m\pi)^2 - (k_x a)^2}, \tag{2}$$
$$y_{ap} = \frac{Y_{11}}{Y_{10}} + 2\sum_{m=3,5}^{\infty} D_m\frac{Y_{1m}}{Y_{10}} + \sum_{m=3,5}^{\infty} D_m^2\left(\frac{Y_{mm}}{Y_{10}} + \frac{Y_{m0}}{Y_{10}}\right).$$

Here, k_y is the Fourier spatial wavenumber, y_{ap} is the normalized aperture admittance, Y_{m0} is the admittance of the generated modes, and D_m can be found by the stationary condition

$$\frac{\partial y_{ap}}{\partial D_m} = 0, \tag{3}$$

The aperture reflection is given by

$$\Gamma = \frac{1 - y_{ap}}{1 + y_{ap}}. \tag{4}$$

Figure 3 shows the effect of the MLA's height on the aperture reflection as a function of frequency. The aperture reflection is calculated by considering three modes. It has been shown that the higher-order modes, with $m > 5$, do not contribute to the aperture reflection [7]. Note that when the height of the aperture decreases, the aperture reflection increases.

5. E-Plane Stepped MLA

Such a high aperture reflection is undesired. In order to match the aperture reflection, and to integrate the MLA with antenna circuits, an air-gap matching network, with two E-plane steps, has been suggested [8]. Using such a technique, the height of the MLA can be reduced, and the integration with a planar antenna circuit will be easier. The reduction of the height can also be achieved by tapering the height. In this case, the configuration is not only complicated to analyze, but the fabrication is also difficult. Figure 4 shows the configuration of the MLA with an air-gap matching network and two E-plane steps.

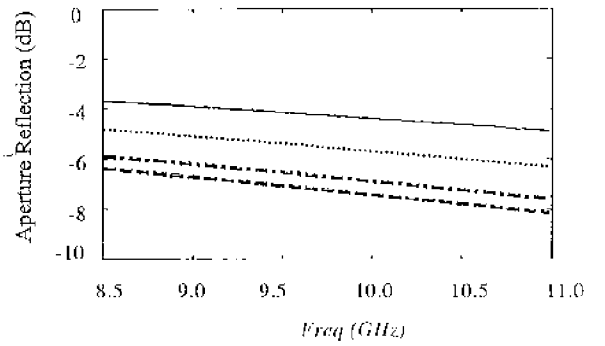

Figure 3. The aperture reflection as a function of frequency, $a = 17$ mm; - - - $b = 6$ mm; ••••• $b = 8$ mm; - • - $b = 10$ mm; ····· $b = 11$ mm.

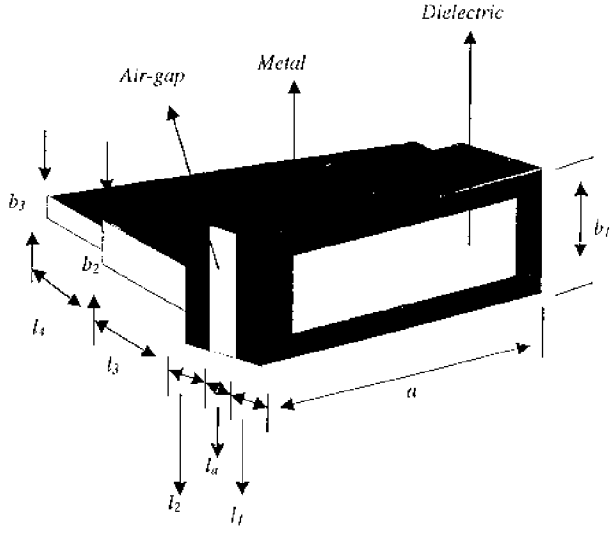

Figure 4a. The MLA with the air-gap matching network and two E-plane steps.

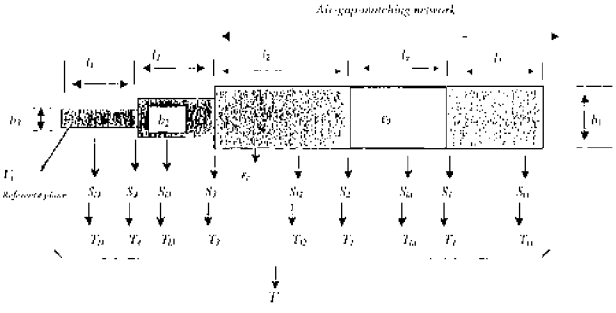

Figure 4b. The MLA with the air-gap matching network and two E-plane steps as a cascaded S-T network.

The air-gap matching network and two E-plane steps are described by a scattering-transmission (S-T) matrix formulation.

6. Input Reflection

The input reflection at the reference plane (see Figure 4) is related to the T matrix of the network and to the aperture reflection by

$$\Gamma_i = \frac{T_{11}\Gamma_a + T_{12}}{T_{21}\Gamma_a + T_{22}}, \tag{5}$$

where the T_{mn} are the elements of the overall T matrix. The overall T-matrix is formed by matrix multiplication, and is given below:

$$T = T_{l4}T_4T_{l3}T_3T_{l2}T_2T_{la}T_1T_{l1} = \begin{bmatrix} T_{11} & T_{12} \\ T_{21} & T_{22} \end{bmatrix}. \tag{6}$$

The scattering matrix of the two-port networks is related to the transmission matrix by

$$T = \begin{bmatrix} T_{11} & T_{12} \\ T_{21} & T_{22} \end{bmatrix} = \begin{bmatrix} -\Delta S & S_{11} \\ -S_{21} & S_{21} \\ -S_{22} & 1 \\ -S_{21} & S_{21} \end{bmatrix}, \tag{7}$$

where $\Delta S = S_{11}S_{22} - S_{21}S_{12}$.

The scattering matrix of the air-gap matching network (see Figure 4) is given in [9]. The scattering matrix is transformed to the transmission matrix using Equation (7), and the related parts are given by

$$T_{lm} = \begin{bmatrix} T_{11} & T_{12} \\ T_{21} & T_{22} \end{bmatrix} = \begin{bmatrix} \exp(-\gamma_m l_m) & 0 \\ 0 & \exp(+\gamma_m l_m) \end{bmatrix},$$

$$T_1 = \frac{1}{2\sqrt{\gamma_a\gamma_1}} \begin{bmatrix} \gamma_a+\gamma_1 & \gamma_a-\gamma_1 \\ \gamma_a-\gamma_1 & \gamma_a+\gamma_1 \end{bmatrix}, \tag{8}$$

$$T_2 = \frac{1}{2\sqrt{\gamma_a\gamma_2}} \begin{bmatrix} \gamma_2+\gamma_a & \gamma_2-\gamma_a \\ \gamma_2-\gamma_a & \gamma_2+\gamma_a \end{bmatrix}.$$

Here, l_m is the length of each homogeneous section (see Figure 4). γ_m is the propagation constant in different sections of the network, and is given by

$$\gamma_m = \begin{cases} j\sqrt{\omega^2\mu_m\varepsilon_m - \left(\dfrac{\pi}{a}\right)^2} & \text{if } \omega^2\mu_m\varepsilon_m \geq \left(\dfrac{\pi}{a}\right)^2, \\ \sqrt{\left(\dfrac{\pi}{a}\right)^2 - \omega^2\mu_m\varepsilon_m} & \text{otherwise.} \end{cases} \tag{9}$$

Here, ω is the frequency, and μ_m and ε_m are the relative permeability and permittivity of the medium, respectively.

The E-plane step configuration, the dimensions, and the lumped-circuit network are shown in Figure 5.

The lumped-circuit network representation is a capacitance, and its susceptance value is given by [10]

$$X_m = Y_{10}\frac{2b_m}{\lambda_g}\left\{\ln\left(\frac{1-s_{m+1}^2}{4s_{m+1}}\right)\left(\frac{1+s_{m+1}}{1-s_{m+1}}\right)^{2\left(s_{m+1}+\frac{1}{s_{m+1}}\right)} + \frac{2}{H_m}\right\},$$

$$\lambda_g = \frac{2\pi}{\gamma_m} = \frac{2\pi}{\sqrt{\omega^2\mu_m\varepsilon_m - \left(\dfrac{\pi}{a}\right)^2}},$$

$$S_m = \frac{b_m}{b_{m-1}}, \tag{10}$$

$$H_m = \left(\frac{1+s_{m+1}}{1-s_{m+1}}\right)^{2s_{m+1}} \frac{1+\sqrt{1-\left(\dfrac{\gamma_m b_m}{2\pi}\right)^2}}{1-\sqrt{1-\left(\dfrac{\gamma_m b_m}{2\pi}\right)^2}} - \frac{1-3s_{m+1}^2}{1-s_{m+1}^2},$$

$$Y_{10} = \frac{\gamma_m}{\omega\mu}, \quad m = 1,2.$$

Here, Y_{10} is the waveguide admittance of the TE_{10} mode, b_{m-1} and b_m are the heights of the steps, λ_g is the wavelength of the dominant mode in the waveguide, and S_m is the step ratio. It has been shown that an accurate result can be achieved by considering the fundamental mode. The transmission-matrix elements of the E-plane step are

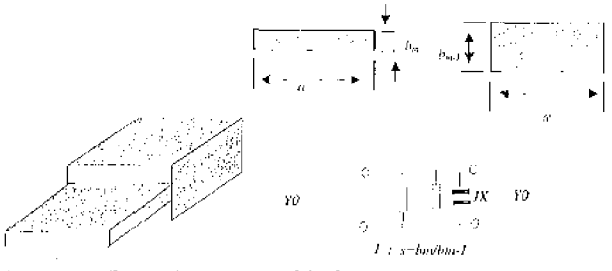

Figure 5. The E-plane step and its lumped-circuit network representation.

$$T_{11}^m = \frac{1+S_{m+1}-jX_m\dfrac{\gamma_m b_m}{\pi}S_{m+1}}{2\sqrt{S_{m+1}}},$$

$$T_{12}^m = \frac{1-S_{m+1}-jX_m\dfrac{\gamma_m b_m}{\pi}S_{m+1}}{2\sqrt{S_{m+1}}},$$

$$T_{21}^m = \frac{1-S_{m+1}+jX_m\dfrac{\gamma_m b_m}{\pi}S_{m+1}}{2\sqrt{S_{m+1}}}, \tag{11}$$

$$T_{22}^m = \frac{1+S_{m+1}+jX_m\dfrac{\gamma_m b_m}{\pi}S_{m+1}}{2\sqrt{S_{m+1}}},$$

$$m = 1,2,$$

where $m = 1,2$ for the first and second steps, respectively. Using Equations (6) and (8) to (11), the elements of the overall transmission matrix are given below:

$$\begin{aligned} T_{11} = \frac{1}{4\gamma_0\sqrt{\gamma_1\gamma_2}}\Big\{&\Big[\left(A_1T_{11}^1A_2T_{11}^2 + A_1T_{12}^1B_2T_{21}^2\right)A_3C \\ &+\left(A_1T_{11}^1A_2T_{12}^2 + A_1T_{12}^1B_2T_{22}^2\right)B_3E\Big]A_4G \\ &+\Big[\left(A_1T_{11}^1A_2T_{11}^2 + A_1T_{12}^1B_2T_{21}^2\right)A_3D \\ &+\left(A_1T_{11}^1A_2T_{12}^2 + A_1T_{12}^1B_2T_{22}^2\right)B_3F\Big]B_4I\Big\}A_5, \end{aligned}$$

$$\begin{aligned} T_{12} = \frac{1}{4\gamma_0\sqrt{\gamma_1\gamma_2}}\Big\{&\Big[\left(A_1T_{11}^1A_2T_{11}^2 + A_1T_{12}^1B_2T_{21}^2\right)A_3C \\ &+\left(A_1T_{11}^1A_2T_{12}^2 + A_1T_{12}^1B_2T_{22}^2\right)B_3E\Big]A_4H \\ &+\Big[\left(A_1T_{11}^1A_2T_{11}^2 + A_1T_{12}^1B_2T_{21}^2\right)A_3D \\ &+\left(A_1T_{11}^1A_2T_{12}^2 + A_1T_{12}^1B_2T_{22}^2\right)B_3F\Big]B_4J\Big\}B_5, \end{aligned} \tag{12}$$

$$\begin{aligned} T_{21} = \frac{1}{4\gamma_0\sqrt{\gamma_1\gamma_2}}\Big\{&\Big[\left(B_1T_{21}^1A_2T_{11}^2 + B_1T_{22}^1B_2T_{21}^2\right)A_3C \\ &+\left(B_1T_{21}^1A_2T_{12}^2 + B_1T_{22}^1B_2T_{22}^2\right)B_3E\Big]A_4G \\ &+\Big[\left(B_1T_{21}^1A_2T_{11}^2 + B_1T_{22}^1B_2T_{21}^2\right)A_3D \\ &+\left(B_1T_{21}^1A_2T_{12}^2 + B_1T_{22}^1B_2T_{22}^2\right)B_3F\Big]B_4I\Big\}A_5, \end{aligned}$$

$$\begin{aligned} T_{22} = \frac{1}{4\gamma_0\sqrt{\gamma_1\gamma_2}}\Big\{&\Big[\left(B_1T_{21}^1A_2T_{11}^2 + B_1T_{22}^1B_2T_{21}^2\right)A_3C \\ &+\left(B_1T_{21}^1A_2T_{12}^2 + B_1T_{22}^1B_2T_{22}^2\right)B_3E\Big]A_4H \\ &+\Big[\left(B_1T_{21}^1A_2T_{11}^2 + B_1T_{22}^1B_2T_{21}^2\right)A_3D \\ &+\left(B_1T_{21}^1A_2T_{12}^2 + B_1T_{22}^1B_2T_{22}^2\right)B_3F\Big]B_4J\Big\}B_5 \end{aligned}$$

where

 1045-9243/00/$10.00© 2000 IEEE

$$T_{11}^1 = \frac{1+S_2 - jB_1 \frac{\gamma_2 b_1}{\pi} S_2}{2\sqrt{S_2}},$$

$$T_{12}^1 = \frac{1-S_2 - jB_1 \frac{\gamma_2 b_1}{\pi} S_2}{2\sqrt{S_2}},$$

$$T_{21}^1 = \frac{1-S_2 + jB_1 \frac{\gamma_2 b_1}{\pi} S_2}{2\sqrt{S_2}},$$

$$T_{22}^1 = \frac{1+S_2 + jB_1 \frac{\gamma_2 b_1}{\pi} S_2}{2\sqrt{S_2}},$$

$$T_{11}^2 = \frac{1+S_3 - jB_2 \frac{\gamma_3 b_2}{\pi} S_3}{2\sqrt{S_3}},$$

$$T_{12}^2 = \frac{1-S_3 - jB_2 \frac{\gamma_3 b_2}{\pi} S_3}{2\sqrt{S_3}},$$

$$T_{21}^2 = \frac{1-S_3 + jB_2 \frac{\gamma_3 b_2}{\pi} S_3}{2\sqrt{S_3}},$$

$$T_{22}^2 = \frac{1+S_3 + jB_2 \frac{\gamma_3 b_2}{\pi} S_3}{2\sqrt{S_3}},$$

$$A_1A_2 = \exp(-\gamma_4 l_4)\exp(-\gamma_3 l_3),$$

$$A_1B_2 = \exp(-\gamma_4 l_4)\exp(+\gamma_3 l_3),$$

$$A_3C = \exp(-\gamma_2 l_2)(\gamma_2 + \gamma_a),$$

$$B_3E = \exp(+\gamma_2 l_2)(\gamma_2 - \gamma_a),$$

$$A_4G = \exp(-\gamma_a l_a)(\gamma_a + \gamma_1),$$

$$A_3D = \exp(-\gamma_2 l_2)(\gamma_2 - \gamma_a),$$

$$B_3F = \exp(+\gamma_2 l_2)(\gamma_2 + \gamma_a),$$

$$B_4I = \exp(+\gamma_a l_a)(\gamma_a - \gamma_1),$$

$$A_4H = \exp(-\gamma_a l_a)(\gamma_a - \gamma_1),$$

$$B_4J = \exp(+\gamma_a l_a)(\gamma_a + \gamma_1),$$

$$B_1A_2 = \exp(+\gamma_4 l_4)\exp(-\gamma_3 l_3),$$

$$B_1B_2 = \exp(+\gamma_4 l_4)\exp(+\gamma_3 l_3),$$

(13)

$$A_5 = \exp(-\gamma_1 l_1),$$

$$B_5 = \exp(+\gamma_1 l_1).$$

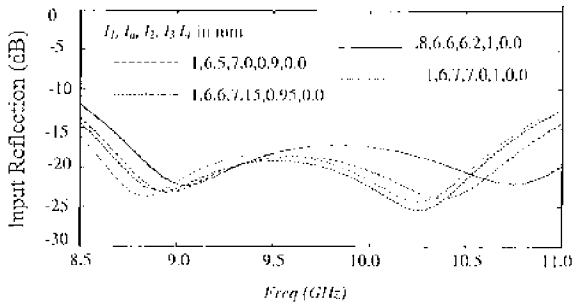

Figure 6. The input reflection as a function of frequency.

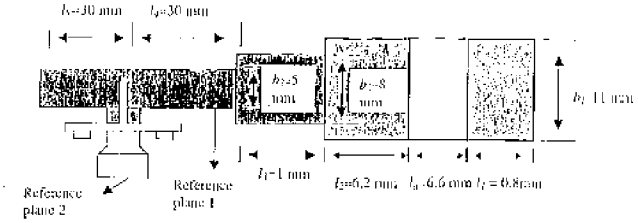

Figure 7. The realized MLA at X band.

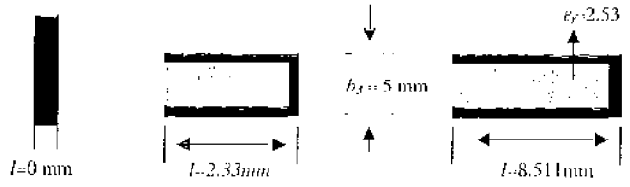

Figure 8. The standard shorts used for waveguide calibration.

Here, $\gamma_1 = \gamma_2 = \gamma_3 = \gamma_4$, since the dielectric constant of the filling material for different sections is the same. Using Equations (5), (9), (10), (12), and (13), the input reflection can be calculated as a function of different parameters. These parameters are the frequency, the dielectric constant, the length of the air gap, and the length of the filled homogeneous section. The design procedure is as follows: the length of the air-gap matching network is chosen such that its reflection coefficient cancels the aperture reflection. Figure 6 shows the input reflection as a function of frequency for different parameters. For this case, $a_1 = a_2 = a_3 = 17$ mm, $b_1 = 11$ mm, $b_2 = 8$ mm, $b_3 = 5$ mm, and $\varepsilon_r = 2.53$. Note that the aperture reflection is calculated using the method given in Section 4. The length of l_4 does not affect the amplitude of the input reflection coefficient. In this case, it only has an effect on the phase. These optimal values are calculated by a trial-and-error method. Note how sensitive the input reflection is to the change in the length of different sections.

7. Measurement Results

Figure 7 shows the realized MLA at X band; $a_1 = a_2 = a_3 = 17$ mm and $\varepsilon_r = 2.53$.

Two different transitions, a coaxial feed and a microstrip end-launcher (MEL), were used to excite the MLA. The analysis and design of the transitions are not presented here, but are presented in references [11-12]. In order to carry out the input reflection measurement at reference plane 1 (see Figure 7), the MLA was calibrated using a Hewlett Packard (HP) modified waveguide calibration. Three standard shorts, with different offset delay, were designed for this purpose. Figure 8 shows the calibration set. The width of the three standards is $a = 17$ mm.

Figure 9 shows the comparison between the calculated and measured input reflection at reference plane 1, as a function of the frequency. The measurement results differ from the theoretical results because the two steps were not implemented in one piece. In order to make a good galvanic contact, it was necessary to use screws. Using such a technique, an air gap can be created between the steps. Also, the influence of the uncertainties in the length of each section were not taken into account. However, it can be seen from Figure 6 how sensitive the input reflection is to the values of the design parameters.

Figure 10 shows the input reflection for two different excitations at reference plane 2. In this case, the MLA measurement was calibrated at reference plane 2 using the HP coax calibration set.

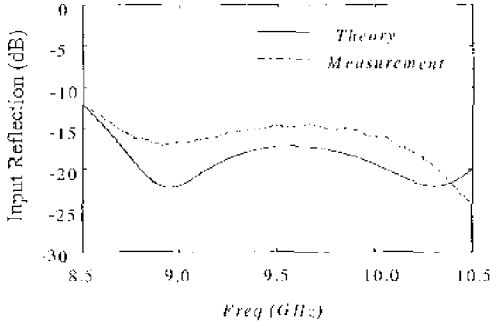

Figure 9. A comparison between the calculated and measured input reflection at reference plane 1.

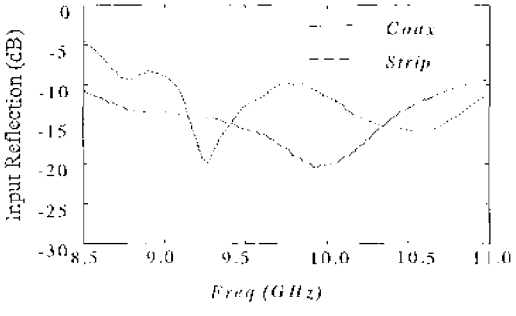

Figure 10. The input reflection as a function of the frequency for two different excitations at reference plane 2.

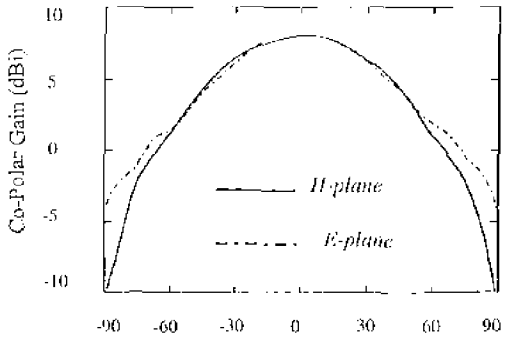

Figure 11a. The co-polar radiation pattern of the MLA at 9.75 GHz.

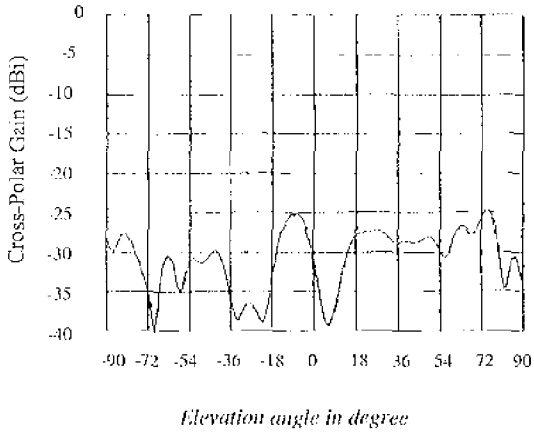

Figure 11b. The cross-polar radiation pattern of the MLA at 9.75 GHz.

For the Collision Avoidance Radar system, the coax transition was used. Figure 11 shows the calibrated E- and H-plane radiation gain patterns of the MLA at 9.75 GHz. The figure also shows the cross-polar radiation gain pattern in the H plane. A maximum gain of 7 dBi and a cross-polarization of less than -25 dBi were achieved. The measurements were performed in an IRCTR anechoic chamber.

8. Conclusions

The analysis of a miniaturized antenna has led to the development of a wideband radiator, with low input reflection over a wide frequency range in the X band. An air-gap matching network was used to reduce high aperture reflection. An input reflection of less than -10 dB over a 1.5 GHz bandwidth was observed. In order to ease the integration with the planar antenna circuit, two E-plane steps were used. A gain of 7 dBi and a cross-polarization of less than -25 dBi were measured. The calculated and measured input-return losses show the practical use of such a design for broadband applications.

9. References

1. D. M. Pozar, "Analysis of an Infinite Array of Rectangular Microstrip Patches with Idealized Probe Feeds," *IEEE Transactions on Antennas and Propagation*, **AP-32**, 1984, pp. 1101-1107.

2. A. B. Smolders and H. J. Visser, "Tracking Phased-Array Antennas in the Netherlands," *Microwaves & RF*, 33, 5, May 1994.

3. C. T. Swift and D. M. Hatcher, "The Input Impedance of a Rectangular Aperture Antenna Loaded with a Dielectric Plug," NASA Technical Note TN D-4430, Washington DC, April 1968.

4. K. J. van Staalduinen, "System Design of a Multistatic FMCW Anti-Collision Radar for Unmanned Vehicles," IRCTR Report S-006 95, Delft University, November 1995.

5. P. J. F. Swart and L. R. Nieuwkerk, "Collision Avoidance Radar Able to Differentiate Objects," *Proceedings of the European Microwave Conference*, Israel, September 1997, pp. 45-50.

6. C. A. S. Balanis, *Antenna Theory, Analysis and Design, Second Edition*, New York, John Wiley & Sons, 1997, Chapter 12.

7. M. Tian, "Characterization of Miniature Dielectric Filled Open Ended Waveguide Antennas," PhD thesis, Delft University, October 1995.

8. M. Hajian and D. P. Tran, "X-Band Microstrip Like Antenna," Internal IRCTR report, February 1995.

9. L. P. Ligthart, "Antenna Design and Characterization Based on the Elementary Antenna Concept," PhD thesis, Dutch Efficiency Bureau, Delft University, 1985.

10. T. Rozzi, "E-Plane Steps in Rectangular Waveguide," *IEEE Transactions on Microwave Theory and Techniques*, **MTT-39**, 8, August 1991.

11. M. Hajian, T. S. Lam, and L. P. Ligthart, "Microstrip-to-Waveguide Transition for Miniature Dielectric-Filled Waveguide Microstrip Like Antennas," *Microwave and Optical Technology Letters*, 2, 5, August 5, 1996, pp. 301-308.

12. M. Hajian and J. E. Giesselbach, "Excitation of Microstrip Like Antenna in X-band," Internal IRCTR report, April 1995.

Introducing Feature Article Authors

M. Hajian was born in Arak, Iran, in 1957. He received his BS in physics from the University of Science and Arts of Oklahoma, USA, 1981, and the MSc(EE) from Delft University of Technology in 1990. Since 1990, he has been with the Microwave and Radar Laboratory of the Delft University of Technology. In 1995, he became a Senior Lecturer, teaching courses in antennas. He is the Netherlands representative to EC/COST 260 on adaptive antennas. His major interests are smart antennas, mobile communication systems for indoors and outdoors, and antenna near-field measurement techniques.

D. P. Tran received the MSc(EE) from the Delft University of Technology, Delft, Netherlands, in 1992. Since 1991, he has served as a researcher at the International Research Centre for Telecommunication Transmissions and Radar (IRCTR). His major interests are antennas and propagation, microwave engineering, and electromagnetic scattering and diffraction.

L. P. Ligthart was born in Rotterdam on September 15, 1946. He graduated with distinction in 1969, and received the MS degree in Electrical Engineering from Delft University of Technology. Since 1969, he has been with the Microwave Laboratory of the Delft University of Technology. In 1974, he became a Senior Lecturer, teaching undergraduate courses in transmission line theory and in antennas and propagation. From 1976 to 1977, he spent one year as a Senior Scientist at Chalmers University, Gothenburg, Sweden. In 1985, he received the PhD in Technical Sciences, based on his contributions to the design of miniaturized waveguide radiating elements.

Prof. Ligthart is Director of IRCTR, covering activities on antennas, propagation, radar, mobile and satellite communications, remote sensing, and electromagnetic compatibility. His present interests include antennas and propagation, radar, and remote sensing. He received the Vederprijs-Award in 1981, the IEE Blumlein Brown Willams Premium award in 1982, and the Doctor Honoris Causa from Moscow State Technical University of Civil Aviation in 1999. He is a Fellow of the IEE, a Senior Member of the IEEE, and the Netherlands representative to EC/COST 260 on adaptive antennas and to EC/COST on advanced weather radar. He has published over 152 scientific papers.